Liquid−Liquid Equilibrium Data for Systems Containing Vegetable Oils, Anhydrous Ethanol, and Hexane at (313.15, 318.15, and 328.15) K

Marcelo Lanza,[†] Guilherme Sanaiotti,[†] Eduardo A. C. Batista,[†] Ronei J. Poppi,[‡] and Antonio J. A. Meirelles*,[†]

ExTrAE, Department of Food Engineering, Faculty of Food Engineering, P.O. Box 6121, University of Campinas - UNICAMP,
13083-862, Campinas, SP, Brazil, and LAQQA, Department of Analytical Chemistry, Chemistry Institute,
P.O. Box 6154, University of Campinas - UNICAMP, 13083-970, Campinas, SP, Brazil

---

The aim of this work was to determine liquid−liquid equilibrium data for systems of interest in ethyl ester (biodiesel) production. The following systems were investigated: refined soybean oil + anhydrous ethanol + hexane at (313.15 ± 0.1) K and (328.25 ± 0.1) K, refined canola oil + anhydrous ethanol + hexane at (313.25 ± 0.1) K and (328.15 ± 0.1) K, and refined palm oil + anhydrous ethanol + hexane at (318.15 ± 0.1) K and (328.25 ± 0.1) K. The instrumental technique of near-infrared spectroscopy allied to multivariate calibration (in this work, this union was denominated "NIR method") was used for quantification of the phase compositions. The NIR method presented an appropriate experimental accuracy for quantifying equilibrium data at higher temperatures. Good reliability of the phase compositions was confirmed from values of global mass balance deviations ranging from (0.06 to 0.16) %. The experimental data were correlated using the NRTL model with an average global deviation of 0.83 %.

Introduction

Almost all energy consumed in the world is provided from petroleum, coal, and natural gas. These sources are limited and with forecast of exhaustion in the future. The concern in relation to this aspect and on ambient questions has generated considerable efforts in the search and development of alternative energy sources, economically viable, ambiently less offensive, and, mainly, renewable. This concern culminated in the insertion of biodiesel in the worldwide energy matrix, particularly in Brazil.[1,2]

Biodiesel is defined as fatty acid alkyl esters produced by alcoholic transesterification reaction of oils and fats, with short-chain alcohols—ethanol or methanol—in the presence of homogeneous (NaOH, KOH, H_2SO_4) or heterogeneous catalysts (enzymes, zeolites, oxides, carbonates, ion-exchange resins). In this reaction, there is still the formation of glycerol as a byproduct.[3]

The conventional transesterification in an industrial scale uses homogeneous acid or base catalysts (NaOH, KOH, H_2SO_4) because they are relatively cheaper and very reactive. On the other hand, their use may also produce undesirable byproducts (such as metallic soaps) whose removal is very difficult, complicating the steps of separation and purification (loss of yield, products of low quality, difficult recovery of glycerol, and large amounts of water used for catalyst removal from the final product).[4−6]

Transesterification can also be catalyzed by enzymes,[7−9] but such a process normally requires the use of organic solvents in which the reagents (oil and ethanol) exhibit relatively high diffusion coefficients. A typical system for biodiesel production using an enzymatic catalyst is composed of oil + ethanol + hexane.[9,10]

The most important factors studied for conduction of the reaction are: use of homogeneous or heterogeneous catalysts, molar ratio of alcohol to oil, temperature, type of alcohol, mainly ethanol or methanol, and type of vegetable oil. One of the most important factors is the temperature. In the case of enzymatic ethanolysis, the reaction is carried out generally in the range of (303.15 to 343.15) K.[2]

Due to the limited mutual solubility of oil and ethanol, knowledge of the phase behavior for systems containing solvents is of the utmost importance for the reactive process because this can influence the reaction path as well as the subsequent purification steps in biodiesel production. For these reasons, it is important to predict the occurrence of one or more liquid phases in the reaction environment and also to be able to estimate the compositions of the phases in equilibrium, as shown in the research of Lanza et al.,[11] Liu et al.,[12] Tizvar et al.,[13] Zhou and Boocock,[14,15] and Zhou et al.[16]

The aim of the present paper was to determine liquid−liquid equilibrium data at different temperatures of (313.15, 318.15, and 328.15) K for fatty systems of interest in biodiesel production, using near-infrared spectroscopy (NIR) coupled with chemometric analysis (multivariate calibration and PLS regression—Partial Least Squares) as the analytical method for quantification of the phase compositions. Near-infrared spectroscopy supplies qualitative data about the samples that can be transformed into quantitative information using chemometric methods based on statistical and mathematical procedures.[17] Reports on the use of NIR spectroscopy in the analysis of vegetable oils and in the determination of liquid−liquid equilibrium data for fatty systems can be found in the literature.[11,18−21]

Experimental Section

Materials. The solvents used in this work were anhydrous ethanol from Merck (Germany), with a purity of 99.9 %, and hexane, also from Merck, with purity greater than 96 %. Refined soybean oil and refined canola oil were purchased from Cargill

---

* Corresponding author. Fax: +55 19 3521 4027. E-mail: tomze@fea.unicamp.br.
[†] Laboratory of Extraction, Applied Thermodynamics and Equilibrium, Faculty of Food Engineering.
[‡] Chemometrics Laboratory in Analytical Chemistry, Chemistry Institute.

10.1021/je800961a CCC: $40.75

Table 1. Fatty Acid Compositions of the Vegetable Oils

fatty acids	symbol	C*x*:y[a]	*M* g·mol^{-1}	refined soybean 100 *w*	refined canola 100 *w*	refined palm 100 *w*
caprylic	Cp	C8:0[a]	144.22			0.08
capric	C	C10:0	172.27			0.09
lauric	L	C12:0	200.32			1.15
myristic	M	C14:0	228.38	0.09	0.07	1.24
palmitic	P	C16:0	256.43	11.18	4.72	40.68
palmitoleic	Po	C16:1	254.42	0.09	0.25	0.15
margaric	Ma	C17:0	270.45			0.10
stearic	S	C18:0	284.49	4.13	2.55	4.72
oleic	O	C18:1	282.47	25.62	62.56	41.78
linoleic	Li	C18:2	280.45	50.88	20.13	8.84
linoelaidic[b]		C18:2T[b]		0.40		0.31
linolenic	Le	C18:3	278.44	4.97	7.08	0.18
translinolenic[b]		C18:3T[b]		1.15	0.41	
arachidic	A	C20:0	312.54	0.45	0.62	0.39
gadoleic	Ga	C20:1	310.52	0.31	1.04	0.15
behenic	Be	C22:0	340.59	0.54	0.28	0.07
lignoceric	Lg	C24:0	368.65	0.19	0.17	0.07
nervonic	Ne	C24:1	366.63		0.12	

[a] C*x*:*y*, *x* = number of carbons and *y* = number of double bonds. [b] Trans isomers.

(Mairinque/SP, Brazil). Refined palm oil was kindly supplied by Agropalma (Belém/PA, Brazil).

The three oils used in this work were analyzed by gas chromatography of the fatty acid methyl esters to determine the fatty acid composition, according to the official method (1−62) of the AOCS.[22] Prior to the chromatographic analysis, the fatty samples were prepared in the form of fatty acid methyl esters according to the method of Hartman and Lago.[23] The vegetable oils were submitted to analysis using a CGC Agilent 6850 Series GC capillary gas chromatograph system under the following experimental conditions: DB-23 Agilent capillary column (50 % cyanopropyl−methylpolysiloxane), 0.25 μm, 60 m × 0.25 mm i.d.; helium as the carrier gas at a rate of 1.0 mL·min^{-1}; linear velocity of 24 cm·s^{-1}; injection temperature of 523.15 K; column temperature of 383.15 K for 5 min, (383.15 to 488.15) K (rate of 5 K·min^{-1}), 488.15 K for 24 min; detection temperature of 553.15 K; and injection volume of 1.0 μL. The fatty acid methyl esters were identified by comparison with external standards purchased from Nu Check Prep (Elysian/MN, USA). Quantification was accomplished by internal normalization.

The fatty acid compositions of the vegetable oils are presented in Table 1, from which the probable triacylglycerol compositions could be determined (Table 2) using the algorithm suggested by Antoniosi Filho et al.[24]

To calculate the probable triacylglycerol compositions, the quantities of trans isomers (see Table 1) were added with their respective cis isomers. In Table 2, the main triacylglycerol represents the component with the greatest composition in the isomer set with *x* carbons and *y* double bonds. The results shown in Tables 1 and 2 allow us to calculate the average molar masses of the refined soybean oil, refined canola oil, and refined palm oil whose values were (873.1, 880.4, and 845.7) g·mol^{-1}, respectively. From the fatty acid compositions of the oils shown in Table 1, the average molar masses of the free fatty acids in each oil were estimated. The values for the average molar masses of the free fatty acids obtained were 278.6 g·mol^{-1} for refined soybean oil, 280.8 g·mol^{-1} for canola oil, and 269.0 g·mol^{-1} for refined palm oil.

Furthermore, the free fatty acid contents of the vegetable oils were determined by titration according to official method 2201 of IUPAC[25] using an automatic buret (Metrohm, model Dosimat 715, Herisan, Switzerland). The free fatty acid mass fractions were 0.11 % for refined soybean oil, 0.09 % for refined canola oil, and 0.08 % for refined palm oil.

Table 2. Probable Triacylglycerol Compositions of the Vegetable Oils

main TAG[a]	group	*M* g·mol^{-1}	refined soybean 100 *w*	refined canola 100 *w*	refined palm 100 *w*
LPP	44:0[b]	751.21			0.49
MPP	46:0	779.27			0.56
LOP	46:1	777.25			1.83
LLiP	46:2	775.24			0.47
PPP	48:0	807.32			4.71
MOP	48:1	805.31			2.05
LOO	48:2	803.29			1.17
PPS	50:0	835.37			1.50
POP	50:1	833.36	1.01	0.50	26.68
PLiP	50:2	831.34	2.08		6.77
POS	52:1	861.41	0.71	0.50	5.81
POO	52:2	859.40	3.91	6.27	23.24
POLi	52:3	857.38	10.30	4.33	9.75
POLe	52:4	855.36		2.32	
PLiLi	52:4	855.36	11.44		1.28
PLiLe	52:5	853.35	2.52	0.59	
POA	54:1	889.46			0.78
SOS	54:1	889.46	0.20		
SOO	54:2	887.45	1.31	3.33	2.68
SOLi	54:3	885.43	5.27		
OOO	54:3	885.43		27.17	6.03
OOLi	54:4	883.42	13.79	25.43	3.41
OLiLi	54:5	881.40	21.86		0.79
OOLe	54:5	881.40		17.21	
OLiLe	54:6	879.38		6.78	
LiLiLi	54:6	879.38	18.11		
LiLiLe	54:7	877.37	5.07		
OLeLe	54:7	877.37		2.05	
LiLeLe	54:8	875.35	0.57		
OOA	56:2	915.50	0.32	0.84	
OOGa	56:3	913.49		1.67	
OLiA	56:3	913.49	0.48		
OLiGa	56:4	911.47		1.01	
LiLiA	56:4	911.47	0.63		
OLiBe	58:3	941.54	0.42		

[a] Groups with a total triacylglycerol (TAG) composition lower than 0.5 % were ignored, except for refined soybean oil. [b] *x*:*y*, *x* = number of carbons (except carbons of glycerol), *y* = number of double bonds.

Apparatus and Procedures. The liquid−liquid equilibrium data for the model systems containing vegetable oil + anhydrous ethanol + hexane were measured at (313.15, 318.15, and 328.15) K. The following oils were tested: refined soybean oil, refined canola oil, and refined palm oil. The liquid−liquid equilibrium data were determined using equilibrium glass cells (50 mL) similar to those used by Silva et al.[26] Known quantities of each component, weighed on an analytical balance with a precision of 0.0001 g (Precisa, model XT220A, Sweden), were added directly inside the equilibrium glass cells. The cell temperature was controlled using a thermostatic bath (Cole Parmer, model 12101-55, Chicago, USA). Digital thermometers (Alla, model 223.15 to 473.15 K, France) with 0.1 K subdivisions were used for monitoring the cell temperature. These digital thermometers were previously calibrated with a standard thermometer in a range of temperatures between (293.15 and 333.15) K. The mixture was stirred vigorously with a magnetic stirrer (Ika Werke, model RH-KT/C, Staufen, Germany) for 20 min and left to rest for (16 to 24) h. This contact time was fixed based on a previous study that showed that phase equilibrium was attained after 2 h of rest.[27] This led to the formation of two clear, transparent phases, with a well-defined interface, and the composition of both phases was measured using the NIR method.

As will be discussed later, the thermodynamic modeling developed in the present manuscript considered the system (vegetable oil + ethanol + hexane) to be a pseudoternary one, replacing the oil by a single triacylglycerol with the average molar mass of the oil. This approach was checked previously by Lanza et al.[11] In this prior work, an overall composition for the pseudoternary system refined soybean oil + anhydrous ethanol + hexane at 298.25 K was selected, and the corresponding liquid−liquid equilibrium data were measured twice. After the analysis of the phases by the NIR method, samples of both phases were evaporated in a vacuum oven (pressure = 75.0 mmHg, temperature = 323.15 K) until complete removal of the solvents, ethanol and hexane. The oil residues of both phases were analyzed by gas chromatography of the fatty acid methyl esters, according to the procedure already described. The results obtained show that, although some triacylglycerols were selectively distributed between both phases, this distribution was restricted to a narrow range of compositions. The average molar masses of the oil residues in both phases were very close to each other, so that the pseudocomponent approach can be considered as approximately valid.

Analytical Method Based on Near Infrared Spectroscopy (NIR). In the present work, the instrumental technique of near-infrared spectroscopy was applied for the quantitative determination of the compounds of the liquid−liquid equilibrium systems. Partial least-squares (PLS) regression was used for the calibration and prediction of the proposed method, employed to obtain relevant information from the complex NIR spectra.[28]

Instrumentation and Software. The near-infrared spectra were measured using a Thermo Nicolet infrared spectrometer (Nexus, model 670 FT-IR Esp, Madison, USA) connected to an air purging system, with a heated cuvette holder (Ventacon, model HNIR-1-1, Winchester, United Kingdom) assisted by a temperature controller (Ventacon, model D-2). Thereby, the NIR spectra could be measured over a large temperature range. After introducing the cuvette in the holder, ca. 3 min was required so that the sample could reach the wished temperature.

Near-infrared absorbance spectra were registered in the range from (4400 to 11000) cm^{-1}, making 64 scans with 4 cm^{-1} resolution using a quartz cell (Hellma, model 110-QX, Müllheim/Baden, Germany) with a 1 mm optical path and 1 cm^{-1} spectra resolution. A spectra of air (empty cell without liquid), obtained before each measured experiment, was used as background. The background spectra (64 scans at 4 cm^{-1} resolution) were recorded to each measure experiment, whereas for the samples, the 64 scans were taken with two repetitions to reduce instrument noise. The calibration methods were developed by PLS regression, available in PLS_Toolbox version 4.0, from Eigenvector Research (Wenatchee, WA, USA) for use with MATLAB 7.0 (The MathWorks, Natick/MA, USA).

Multivariate Calibration. To develop calibration models appropriate for each system, sets of mixtures with compositions close to the binodal curve were selected. Each binodal curve was divided into two parts, the oil phase and the alcoholic phase, and for each part, 30 pseudoternary mixtures were obtained by gravimetry and used as calibration standards. On the basis of these sets and the near-infrared spectra, the PLS regression generated the calibration models. A further set of about 10 pseudoternary mixtures for each part of the binodal curve was also obtained by gravimetry and used as an external validation set (prediction set) to check the accuracy of the calibration models. The compositions of the calibration and external validation standards were selected using a binodal curve previously determined by the cloud-point method or estimated using calibration models for fatty systems containing soybean or canola oils at a lower temperature previously determined by Lanza et al.[11]

For the cloud-point method, measurements were performed according to the selected temperature in glass cells (50 mL) containing vegetable oil and ethanol in the composition range from 20 % to 90 % in mass of ethanol. Mixtures in this composition range generate two liquid phases. Using an automatic buret (Metrohm, model Dosimat 715, Herisan, Switzerland), hexane was added to the glass cells under vigorous agitation, until the appearance of a single homogeneous liquid phase. The corresponding binodal curve was calculated using the added amount of each component. All measurements were accomplished in glass cells under temperature control by a thermostatic bath. A magnetic stirrer was used to promote the necessary agitation, and digital thermometers (Alla, model 223.15 to 473.15 K, France) with 0.1 K subdivisions were used for monitoring the mixture temperature.

The accuracy of the calibration models was evaluated by the relative error (E_R), obtained from the difference between the predicted and the actual values (gravimetry), the coefficient of determination (R^2), the linear plot between the predicted values and the actual ones, and the root-mean-square error (rmse). These values express the accuracy of the models and the proximity between the values predicted by the model ($w_{i,\text{pred}}$) and the actual values ($w_{i,\text{actual}}$) obtained using the reference method. The errors were defined as

$$E_R = \frac{1}{n}\sum_{i=1}^{n}\frac{|w_{i,\text{pred}} - w_{i,\text{actual}}|}{w_{i,\text{actual}}} \tag{1}$$

$$\text{rmse} = \sqrt{\frac{\sum_{i=1}^{n}(w_{i,\text{pred}} - w_{i,\text{actual}})^2}{n}} \tag{2}$$

where n is the total number of samples and the subscript i is the number of the sample.

The rmsec (root-mean-square error of calibration) is the rmse calculated using the calibration standards (internal validation). The rmsecv (root-mean-square error of cross-validation) is the rmse calculated using the cross-validation standards (internal validation), according to the cross-validation procedure known as "leave one out".[29,30] The cross-validation procedure through

Table 3. Errors in the Quantification of the Validation Standards (Internal and External) for the System Containing Refined Soybean Oil (1) + Anhydrous Ethanol (4) + Hexane (5) at (313.15 ± 0.1) K and (328.25 ± 0.1) K Using the NIR Method

		alcoholic phase			oil phase			
T/K		oil (1)	ethanol (4)	hexane (5)	oil (1)	ethanol (4)	hexane (5)	E_R/%
313.15 ± 0.1	E_R/%	0.68	0.15	1.81	0.20	0.49	1.58	0.82
	rmsep/%	0.11	0.13	0.11	0.18	0.15	0.10	
	rmsec/%	0.08	0.05	0.08	0.28	0.21	0.07	
	rmsecv/%	0.12	0.07	0.12	0.34	0.29	0.10	
	R^2	0.99961	0.99998	0.99953	0.99963	0.99922	0.99974	
328.25 ± 0.1	E_R/%	1.42	0.32	4.03	0.39	0.87	2.57	1.60
	rmsep/%	0.43	0.42	0.10	0.32	0.32	0.04	
	rmsec/%	0.18	0.22	0.02	0.49	0.47	0.02	
	rmsecv/%	0.35	0.28	0.06	0.72	0.71	0.06	
	R^2	0.99406	0.99610	0.99217	0.99646	0.99417	0.99853	

their corresponding rmsecv values and the relative errors (E_R) between the predicted and the actual values of the external validation standards were used for selecting the number of PLS factors considered in the construction of the calibration models. The rmsep (root-mean-square error of prediction) is the rmse calculated using the external validation standards, a special set of standards not included in the construction of the calibration models (external validation). After determining and checking the calibration models for each phase, oil or alcoholic, of each system, these models could be used to calculate the compositions of the samples obtained in the equilibrium experiments. The uncertainties of the compositions for the NIR method varied within the following ranges: (0.04 to 0.60) % for oil, (0.02 to 0.66) % for ethanol, and (0.05 to 0.14) % for hexane, being the lowest figures obtained for the lowest compositions.

Theoretical Calculations

Calculation of the Deviations in the Mass Balance of the Phases. To test the accuracy and reliability of the equilibrium data, the procedure developed by Marcilla et al.,[31] and already applied to fatty systems by Rodrigues et al.,[27,32] was followed. This procedure consists of calculating the masses for both liquid phases and comparing their sum with the actual value for total mass used in the experiment, thus obtaining a relative error for each experimental result for an overall mixture. According to this approach, i independent component balances can be written, with i being each component of the system, given by

$$m^{OC}w_i^{OC} = m^{AP}w_i^{AP} + m^{OP}w_i^{OP} \tag{3}$$

where m^{OC} is the mass amount of the overall composition (initial mixture); m^{AP} and m^{OP} are the masses of the alcoholic and oil phases, respectively; w_i^{OC} is the mass fraction of component i in the initial mixture; and $w_i^{AP}$and w_i^{OP} are the mass fractions of component i in the alcoholic and oil phases, respectively. With these i equations, it is possible to calculate the values for m^{AP} and m^{OP} from the experimental values w_i^{AP} and w_i^{OP} using a least-squares fitting. If **M** is the matrix formed by the values for w_i^{OC}, **B** is the transformation matrix (formed by the values for w_i^{AP} and w_i^{OP}), and **P** is the matrix formed by the mass of each phase (m^{AP} and m^{OP}), the previous system can be written as

$$\mathbf{M} = \mathbf{B}\cdot\mathbf{P} \tag{4}$$

Mathematical calculations transform eq 4 into the following expression

$$\mathbf{P} = (\mathbf{B}^{T}\mathbf{B})^{-1}\mathbf{B}^{T}\mathbf{M} \tag{5}$$

where $\mathbf{B}^T$ is the transpose matrix of **B** and $(\mathbf{B}^T\mathbf{B})^{-1}$ is the inverse matrix of $(\mathbf{B}^T\mathbf{B})$. In this way, the values for m^{AP} and m^{OP} (matrix **P**), which minimize the errors of the previous system, have been calculated. The sum of m^{AP} and m^{OP} can be compared to m^{OC} to estimate relative deviation for the overall mass balance (δ), expressed as

$$\delta = \frac{|(m^{AP} + m^{OP}) - m^{OC}|}{m^{OC}} \tag{6}$$

The relative deviation for mass balance of each compound i (δ_i) in each tie line n could be calculated according to eq 7

$$\delta_{i,n} = \frac{|m_n^{OC}w_{i,n}^{OC} - (m_n^{AP}w_{i,n}^{AP} + m_n^{OP}w_{i,n}^{OP})|}{m_n^{OC}w_{i,n}^{OC}} \tag{7}$$

The relative deviations for each compound (δ_i) varied within the following ranges: (0.01 to 0.07) % for oil, (0.01 to 0.05) % for ethanol, and (0.19 to 12.58) % for hexane, being the lowest values obtained for the largest compositions. As indicated above, the mass balance deviations for hexane varied over a larger range in comparison to the other components. The reason for that behavior is that hexane is always a minor component in the present systems, with fractions varying within the range 0.0033 to 0.1034. In this case, small absolute deviations may generate some large relative deviations for component mass balance. Nevertheless, the average relative deviation for the hexane mass balance in the whole set of experimental data was 3.90 %. The relative deviation for the overall mass balance, calculated according to eq 6, was lower than 0.2 %, with an average value of 0.09 %, confirming the high quality of the experimental data.[31]

Thermodynamic Modeling. The concept of local composition basically establishes that the composition of the system in the neighborhood of a given molecule is not the same as the "bulk" composition because of intermolecular forces.[33] The NRTL (nonrandom, two-liquid) model developed by Renon and Prausnitz[34] for the activity coefficient is based on the local composition concept, and it is applicable to partially miscible systems.[35,36]

Mole fractions have been traditionally used in this model, but mass fractions is a more convenient composition unit due to the large difference in the molar masses of components such as vegetable oils, ethanol, and hexane. Several investigations used this approach with the NRTL model.[11,27,32,35−37] In the case of using mass fractions, the NRTL model for multicomponent mixtures is expressed as

$$\ln \gamma_i^w = \left(\frac{\sum_{j=1}^{K} \frac{\tau_{ji} G_{ji} w_j}{\bar{M}_j}}{\sum_{j=1}^{K} \frac{G_{ji} w_j}{\bar{M}_j}} + \sum_{j=1}^{K} \left[\frac{w_j G_{ij}}{\bar{M}_j \sum_{k=1}^{K} \frac{G_{kj} w_k}{\bar{M}_k}} \left(\tau_{ij} - \frac{\sum_{k=1}^{K} \frac{\tau_{kj} G_{kj} w_k}{\bar{M}_k}}{\sum_{k=1}^{K} \frac{G_{kj} w_k}{\bar{M}_k}} \right) \right] \right) \Big/ \bar{M}_i \sum_{j=1}^{K} \left(\frac{w_j}{\bar{M}_j} \right) \tag{8}$$

where

$$\tau_{ij} = \frac{\Delta g_{ij}}{RT} \tag{9}$$

$$\frac{\Delta g_{ij}}{R} = A_{0,ij} + A_{1,ij} T \tag{10}$$

$$G_{ij} = \exp(-\alpha_{ij} \tau_{ij}) \tag{11}$$

$$\alpha_{ij} = \alpha_{ji} \tag{12}$$

where γ_i^w is the corresponding activity coefficient of component i expressed on the mass fraction scale; $\bar{M}$ and w are average molar mass and mass fraction, respectively, of the pseudo components; Δg_{ij} and τ_{ij} represent the molecular energy interactions between the components $i-j$; α_{ij} is the parameter of nonrandomness of the mixture which means that the components are distributed in a pattern dictated by the local composition; T is the absolute temperature; and $A_{0,ij}$, $A_{0,ji}$, $A_{1,ij}$, and $A_{1,ji}$ are characteristic energy parameters of the $i-j$ interactions. Thus, in the present case, there are five adjustable parameters for each pair of substances. These parameters can be estimated with experimental data, by using the procedure below. When the data are at the same temperature or the number of points is small and there is not enough information, the extended NRTL model reduces to the original NRTL[34] model and hence the $A_{1,ij}$ and $A_{1,ji}$ terms of eq 10 vanish.[35,36]

The experimental data for the system refined soybean oil + anhydrous ethanol + hexane at 298.15 K and refined canola oil + anhydrous ethanol + hexane at 298.15 K determined by Lanza et al.[11] were used with experimental data determined in this work, at (313.15, 318.15, and 328.15) K, to adjust the temperature-dependent parameters (eq 10) of the NRTL model.

Adjustment was done by treating the system vegetable oil + anhydrous ethanol + hexane as a pseudoternary one. For the adjustment process, the vegetable oil was treated as a single triacylglycerol with the average molar mass of the oil. This approach assumes that the different triacylglycerols present in the vegetable oil behave in a very similar way in the liquid−liquid system under analysis. In this case, such compounds can be adequately replaced by a pseudocomponent having the corresponding average physical-chemical properties. This approach was already evaluated by Lanza et al.,[11] which proved the reliability of this hypothesis.

The calculation of the activity coefficients and the estimation of parameters were performed using a computational program developed in Fortran language by Stragevitch.[37] In the present work, all five parameters corresponding to each binary mixture were adjusted to the experimental data, including the α_{ij} values. The adjustment of the α_{ij} values allowed a better correlation of the equilibrium data and is an approach already used in the literature.[38−41]

Estimation of the parameters was based on minimization of the objective function of compositions, eq 13, following the procedure developed by Stragevitch and d'Avila.[42]

$$\mathrm{OF}(w) = \sum_{m}^{D} \sum_{n}^{N} \sum_{i}^{K-1} \left[\left(\frac{w_{i,n,m}^{\mathrm{AP,exptl}} - w_{i,n,m}^{\mathrm{AP,calcd}}}{\sigma_{w_{i,n,m}^{\mathrm{AP}}}} \right)^2 + \left(\frac{w_{i,n,m}^{\mathrm{OP,exptl}} - w_{i,n,m}^{\mathrm{OP,calcd}}}{\sigma_{w_{i,n,m}^{\mathrm{OP}}}} \right)^2 \right] \tag{13}$$

where D is the total number of data groups; N is the total number of tie lines; K is the total number of pseudocomponents in the data group; w is the mass fraction; the subscripts i, n, and m are component, tie line, and group number, respectively; the superscripts AP and OP stand for the alcoholic and oil phases, respectively; and exptl and calcd refer to experimental and calculated compositions. $\sigma_{w_{i,n,m}^{\mathrm{AP}}}$ and $\sigma_{w_{i,n,m}^{\mathrm{OP}}}$ are the standard deviations observed in the compositions of the two liquid phases.

According to the program developed by Stragevitch,[37] the parameter estimation procedure and the calculation of the compositions for minimization of the objective function, eq 13, are done by liquid−liquid flash calculations, and the middle point compositions of the experimental tie lines are used as the feed composition.[43] The average deviations between the experimental and calculated compositions in both phases were calculated according to eq 14.

$$\Delta w = \sqrt{\frac{\sum_{n}^{N} \sum_{i}^{K} [(w_{i,n}^{\mathrm{AP,exptl}} - w_{i,n}^{\mathrm{AP,calcd}})^2 + (w_{i,n}^{\mathrm{OP,exptl}} - w_{i,n}^{\mathrm{OP,calcd}})^2]}{2NK}} \tag{14}$$

Results and Discussion

As explained in our prior work,[11] the use of the NIR spectroscopy for quantifying the phase compositions requires the development of calibration models. Such models are developed on the basis of mixtures with known compositions located in the vicinity of the binodal curve, and in the case of systems containing soybean oil or canola oil, the corresponding calibration models at 298.15 K were already available.[11] For this reason, a first attempt was done to evaluate if those calibration models were appropriate for higher temperatures [(313.15 or 328.15) K]. Equilibrium experiments were conducted, according to the procedure described above, for systems containing soybean or canola oils + ethanol + hexane at (313.15 and 328.15) K. Phase samples were collected, and the corresponding NIR spectra were measured, stored, and evaluated using the calibration models developed at 298.15 K. Unfortunately, the obtained equilibrium using the prior calibration models were not accurate enough, with large deviations according to the mass balance evaluation by the procedure suggested by Marcilla et al.[28] Despite this fact, such not highly accurate equilibrium data allowed the estimation of binodal curves, and with the additional help of a limited set of cloud-point experiments, it was possible to select sets of calibration standards at (313.15 and 328.15) K so that new calibration

Table 4. Errors in the Quantification of the Validation Standards (Internal and External) for the System Containing Refined Canola Oil (2) + Anhydrous Ethanol (4) + Hexane (5) at (313.25 ± 0.1) K and (328.15 ± 0.1) K Using the NIR Method

		alcoholic phase			oil phase			
T/K		oil (2)	ethanol (4)	hexane (5)	oil (2)	ethanol (4)	hexane (5)	E_R/%
313.25 ± 0.1	E_R/%	0.37	0.04	1.57	0.13	0.82	2.34	0.88
	rmsep/%	0.05	0.04	0.08	0.13	0.21	0.16	
	rmsec/%	0.03	0.07	0.03	0.14	0.10	0.05	
	rmsecv/%	0.09	0.12	0.07	0.19	0.16	0.08	
	R^2	0.99990	0.99997	0.99948	0.99959	0.99927	0.99964	
328.15 ± 0.1	E_R/%	1.29	0.29	1.85	0.85	2.18	3.93	1.73
	rmsep/%	0.28	0.27	0.05	0.77	0.79	0.12	
	rmsec/%	0.05	0.07	0.02	1.24	1.11	0.08	
	rmsecv/%	0.11	0.10	0.05	1.96	1.77	0.22	
	R^2	0.99881	0.99929	0.99917	0.99340	0.98726	0.99881	

Table 5. Errors in the Quantification of the Validation Standards (Internal and External) for the System Containing Refined Palm Oil (3) + Anhydrous Ethanol (4) + Hexane (5) at (318.15 ± 0.1) K and (328.25 ± 0.1) K Using the NIR Method

		alcoholic phase			oil phase			
T/K		oil (3)	ethanol (4)	hexane (5)	oil (3)	ethanol (4)	hexane (5)	E_R/%
318.15 ± 0.1	E_R/%	0.84	0.07	1.13	0.67	1.47	1.65	0.97
	rmsep/%	0.08	0.07	0.09	0.53	0.44	0.17	
	rmsec/%	0.18	0.15	0.08	0.66	0.70	0.09	
	rmsecv/%	0.27	0.21	0.14	1.41	1.43	0.12	
	R^2	0.99969	0.99997	0.99905	0.99499	0.99079	0.99866	
328.25 ± 0.1	E_R/%	0.75	0.15	5.70	0.46	0.83	2.67	1.76
	rmsep/%	0.12	0.15	0.11	0.35	0.33	0.05	
	rmsec/%	0.04	0.09	0.05	0.25	0.25	0.01	
	rmsecv/%	0.12	0.12	0.09	0.35	0.36	0.03	
	R^2	0.99903	0.99920	0.99344	0.99834	0.99724	0.99941	

Table 6. Liquid−Liquid Equilibrium Data for the Pseudoternary System Containing Refined Soybean Oil (1) + Anhydrous Ethanol (4) + Hexane (5) at (313.15 ± 0.1) K and (328.25 ± 0.1) K

	overall composition			alcoholic phase			oil phase		
T/K	100 w_1	100 w_4	100 w_5	100 w_1	100 w_4	100 w_5	100 w_1	100 w_4	100 w_5
313.15 ± 0.1	50.08	49.92	0.00	9.42	90.58	0.00	78.60	21.40	0.00
	48.85	50.04	1.11	10.94	88.18	0.88	75.95	22.75	1.30
	47.49	50.11	2.40	11.30	86.46	2.24	74.30	23.17	2.53
	46.23	50.06	3.71	13.34	83.39	3.27	71.12	24.99	3.89
	45.08	50.08	4.84	13.56	81.94	4.50	70.03	25.08	4.89
	44.01	50.06	5.93	15.81	78.89	5.30	66.33	27.65	6.02
	43.00	50.00	7.00	16.29	77.05	6.66	64.24	28.36	7.40
	41.95	50.06	7.99	18.30	74.24	7.46	61.63	30.14	8.23
	41.14	50.32	8.54	20.32	71.53	8.15	59.00	32.09	8.91
	41.08	50.03	8.89	20.24	71.04	8.72	57.92	32.59	9.49
	40.13	50.08	9.79	22.99	67.33	9.68	55.44	34.36	10.20
328.25 ± 0.1	49.95	50.05	0.00	15.88	84.12	0.00	66.56	33.44	0.00
	49.49	50.00	0.51	16.24	83.43	0.33	65.76	33.73	0.51
	48.99	50.01	1.00	18.71	80.44	0.85	64.42	34.62	0.96
	48.49	50.00	1.51	20.18	78.63	1.19	62.70	35.91	1.39
	47.99	50.00	2.01	21.88	76.39	1.73	60.33	37.73	1.94
	47.50	50.01	2.49	24.26	73.35	2.39	57.46	39.98	2.56
	46.99	50.00	3.01	25.58	71.53	2.89	53.94	43.03	3.03

models for the systems with soybean or canola oils were developed. In the case of palm oil, for which no prior calibration model was available, binodal curves were determined by the cloud point method at the selected temperatures and the corresponding calibration standards chosen. It is worth mentioning that it was not possible to determine liquid−liquid equilibrium data involving refined palm oil at temperatures lower than 318.15 K because this oil has a melting point at about 309.15 K and is in solid form at room temperature.[44] Furthermore, all calibration models were checked against sets of external validation standards so that a whole set of reliable models for evaluating the phase compositions was determined, one model for each pseudocomponent in the oil and alcoholic phases at each selected temperature.

Tables 3, 4, and 5 show the results of the calibration models generated through NIR spectroscopy for the three different fatty systems, containing soybean, canola, or palm oils. As can be seen in these tables, the calibration models exhibit high coefficients of determination (R^2) and low values for root-mean-square errors of prediction, calibration, and cross-validation (rmsep, rmsec, and rmsecv). It can also be observed that the errors present a slight increase with the temperature, particularly for hexane. The temperature increase diminishes the region of phase splitting, decreasing the range of fractions for hexane. The errors are also slightly larger for components in low fractions, such as oil in the alcoholic phase and ethanol in the oil phase. In fact, for low fractions, the relative deviations are usually larger.

Tables 6, 7, and 8 show the overall experimental composition and the corresponding tie lines for fatty systems containing soybean, canola, or palm oils. The pseudocomponents used in this work received the following notations: refined soybean oil (1), refined canola oil (2), refined palm oil (3), anhydrous ethanol (4), and hexane (5).

The experimental data measured in this work at (313.15, 318.15, and 328.15) K and those determined by Lanza et al.[11]

Table 7. Liquid−Liquid Equilibrium Data for the Pseudoternary System Containing Refined Canola Oil (2) + Anhydrous Ethanol (4) + Hexane (5) at (313.25 ± 0.1) K and (328.15 ± 0.1) K

	overall composition			alcoholic phase			oil phase		
T/K	100 w_2	100 w_4	100 w_5	100 w_2	100 w_4	100 w_5	100 w_2	100 w_4	100 w_5
313.25 ± 0.1	50.00	50.00	0.00	8.96	91.04	0.00	79.69	20.31	0.00
	48.76	49.96	1.28	9.71	88.89	1.40	77.42	21.30	1.28
	47.49	49.99	2.52	10.64	86.82	2.54	76.56	20.75	2.69
	46.67	49.47	3.86	11.29	84.98	3.73	72.80	23.01	4.19
	44.99	49.99	5.02	12.37	82.88	4.75	70.84	24.09	5.07
	43.73	50.00	6.27	13.82	80.27	5.91	68.15	25.49	6.36
	42.50	49.98	7.52	14.97	77.76	7.27	64.64	27.35	8.01
	41.24	50.01	8.75	17.00	74.53	8.47	61.44	29.41	9.15
	40.00	50.00	10.00	19.28	71.01	9.71	58.03	31.63	10.34
328.15 ± 0.1	45.00	55.00	0.00	15.34	84.66	0.00	71.06	28.94	0.00
	44.40	54.99	0.61	17.08	82.45	0.47	69.72	29.49	0.79
	43.79	55.00	1.21	17.15	81.82	1.03	67.92	30.69	1.39
	43.20	54.99	1.81	17.79	80.51	1.70	67.12	31.12	1.76
	42.60	55.01	2.39	19.19	78.72	2.09	65.25	32.24	2.51
	41.99	55.01	3.00	21.60	75.72	2.68	63.00	33.86	3.14
	41.40	54.98	3.62	23.54	73.14	3.32	61.02	35.52	3.46
	40.81	54.99	4.20	26.25	69.95	3.80	55.95	39.97	4.08

Table 8. Liquid−Liquid Equilibrium Data for the Pseudoternary System Containing Refined Palm Oil (3) + Anhydrous Ethanol (4) + Hexane (5) at (318.15 ± 0.1) K and (328.25 ± 0.1) K

	overall composition			alcoholic phase			oil phase		
T/K	100 w_3	100 w_4	100 w_5	100 w_3	100 w_4	100 w_5	100 w_3	100 w_4	100 w_5
318.15 ± 0.1	49.98	50.02	0.00	11.37	88.63	0.00	78.37	21.63	0.00
	49.06	50.00	0.94	12.24	86.88	0.88	76.97	21.99	1.04
	48.10	49.99	1.91	13.28	85.07	1.65	75.98	22.16	1.86
	47.16	49.98	2.85	13.49	84.01	2.50	72.43	24.77	2.80
	46.20	50.01	3.79	14.65	81.93	3.42	69.89	26.47	3.64
	45.25	50.01	4.74	16.10	79.82	4.08	67.96	27.32	4.72
	44.28	50.03	5.69	16.86	78.07	5.07	65.86	28.51	5.63
328.25 ± 0.1	39.99	60.01	0.00	16.65	83.35	0.00	68.92	31.08	0.00
	39.49	60.00	0.51	18.25	81.31	0.44	67.25	32.18	0.57
	39.00	59.98	1.02	18.99	80.15	0.86	66.46	32.51	1.03
	38.48	60.02	1.50	19.19	79.28	1.53	65.40	33.03	1.57
	37.98	59.99	2.03	20.77	77.24	1.99	63.07	34.86	2.07
	37.52	59.98	2.50	22.16	75.58	2.26	61.56	36.03	2.41
	36.97	60.01	3.02	21.65	75.53	2.82	61.25	35.71	3.04
	36.51	59.99	3.50	24.74	71.92	3.34	58.40	38.07	3.53
	36.01	59.98	4.01	26.93	69.15	3.92	55.87	40.11	4.02

Table 9. Temperature-Dependent NRTL Parameters

pair ij[a]	$A_{0,ij}$/K	$A_{0,ji}$/K	$A_{1,ij}$	$A_{1,ji}$	α_{ij}
14	2592.5	−12.56	−9.698	5.731	0.3761
15	−7.99	2856.0	−2.7874	−8.27	0.3313
24	3063.9	−1517.9	−12.41	12.56	0.2363
25	−2572.6	2595.7	5.78	−7.0	0.3008
34	4240.5	−2651.5	−16.07	15.961	0.2325
35	−154.53	1959.2	−2.642	−4.14	0.2587
45	5789.0	−22046.0	−18.365	74.067	0.2720

[a] Refined soybean oil (1), refined canola oil (2), refined palm oil (3), anhydrous ethanol (4), and hexane (5).

Table 10. Mean Deviations in Phase Compositions for Systems Containing Vegetable Oil (Soybean, Canola, or Palm) + Anhydrous Ethanol + Hexane at Different Temperatures

	T/K				
oil	298.15[a]	313.15	318.15	328.15	100 Δw
refined soybean	0.47	0.60		0.79	0.60
refined canola	1.00	0.47		1.40	1.01
refined palm			1.00	0.73	0.86
average overall deviation					0.83

[a] Mean deviations calculated for data taken from Lanza et al.[11]

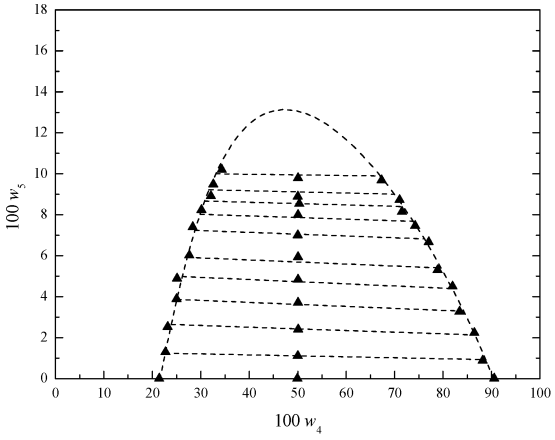

Figure 1. Liquid−liquid equilibrium for the system containing refined soybean oil (1) + anhydrous ethanol (4) + hexane (5) at (313.15 ± 0.1) K: ▲, experimental; ---, NRTL model.

for the systems refined soybean oil + anhydrous ethanol + hexane at 298.15 K and refined canola oil + anhydrous ethanol + hexane at 298.15 K were used to adjust the NRTL temperature-dependent parameters presented in Table 9. The average deviations between the experimental and calculated compositions according to eq 14 are presented in Table 10.

Figures 1 and 2 show the experimental points, tie lines, and binodal curves calculated using the NRTL model for the system containing refined soybean oil (1) + anhydrous ethanol (4) + hexane (5) at (313.15 ± 0.1) K and (328.25 ± 0.1) K, respectively. The selected thermodynamic model was able to accurately describe the phase compositions, as can be further

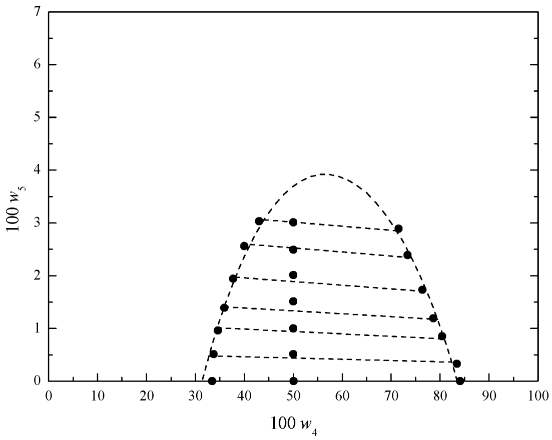

Figure 2. Liquid−liquid equilibrium for the system containing refined soybean oil (1) + anhydrous ethanol (4) + hexane (5) at (328.25 ± 0.1) K: ●, experimental; ---, NRTL model.

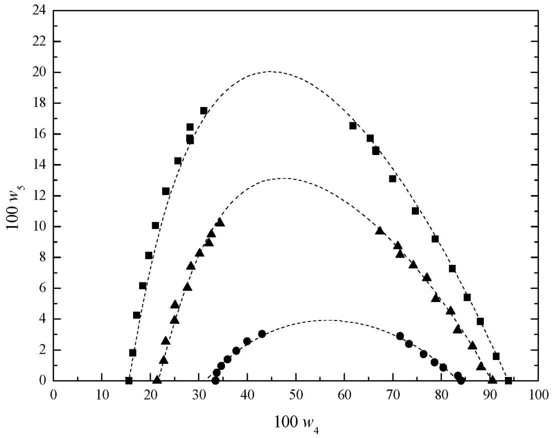

Figure 3. Liquid−liquid equilibrium for the system containing refined soybean oil (1) + anhydrous ethanol (4) + hexane (5) at (298.25, 313.15, and 328.25) K: ■, experimental data at (298.25 ± 0.2) K taken from ref 11; ▲, experimental data at (313.15 ± 0.1) K obtained in this work; ●, experimental data at (328.25 ± 0.1) K obtained in this work; ---, binodal curves calculated by the NRTL model in this work.

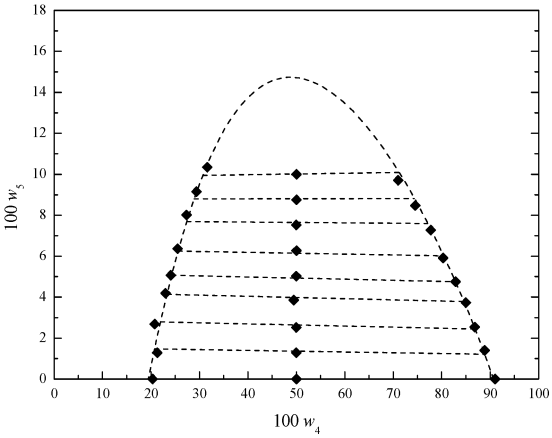

Figure 4. Liquid−liquid equilibrium for the system containing refined canola oil (2) + anhydrous ethanol (4) + hexane (5) at (313.25 ± 0.1) K: ♦, experimental; ---, NRTL model.

confirmed by the corresponding low deviation (0.60 and 0.79) %, respectively, presented in Table 10. The global mass balance deviation for the systems containing soybean oil at (313.15 and 328.25) K, evaluated according to the procedure suggested by Marcilla et al.,[28] were (0.09 and 0.07) %, respectively, values which indicate the good quality of the experimental data.

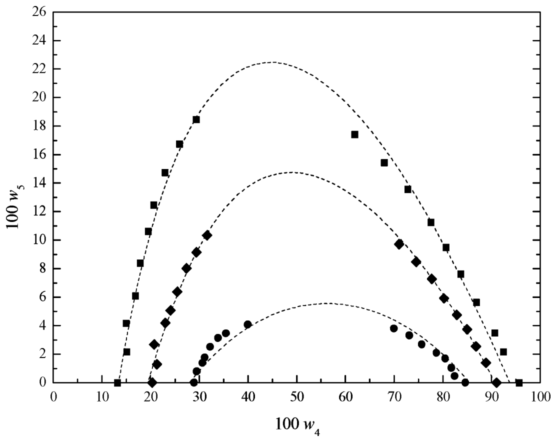

Figure 5. Liquid−liquid equilibrium for the system containing refined canola oil (1) + anhydrous ethanol (4) + hexane (5) at (298.25, 313.25, and 328.15) K: ■, experimental data at (298.25 ± 0.2) K taken from ref 11; ♦, experimental data at (313.25 ± 0.1) K obtained in this work; ● experimental data at (328.15 ± 0.1) K obtained in this work; ---, binodal curves calculated by the NRTL model in this work.

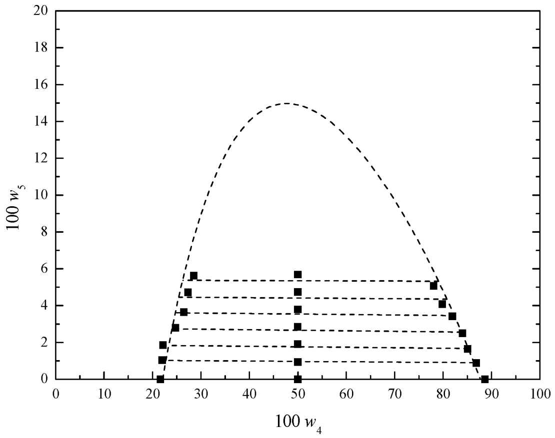

Figure 6. Liquid−liquid equilibrium for the system containing refined palm oil (3) + anhydrous ethanol (4) + hexane (5) at (318.15 ± 0.1) K: ■, experimental; ---, NRTL model.

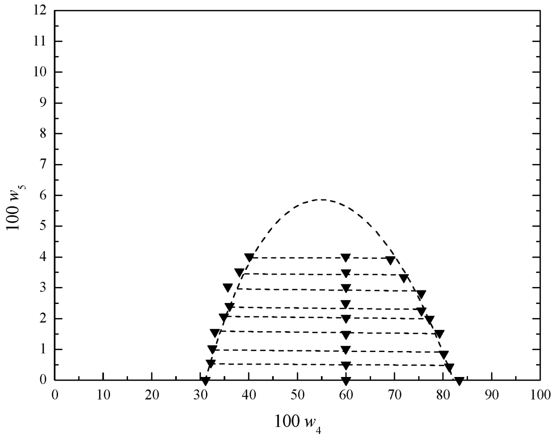

Figure 7. Liquid−liquid equilibrium for the system containing refined palm oil (3) + anhydrous ethanol (4) + hexane (5) at (328.25 ± 0.1) K: ▼, experimental; ---, NRTL model.

To compare results for the system containing refined soybean oil + anhydrous ethanol + hexane at the three different temperatures, the corresponding experimental equilibrium data and binodal curves calculated by the NRTL model are shown in Figure 3.

As can be seen in Figure 3, increasing temperature decreases the immiscibility region, so that lower amounts of hexane are required to avoid oil−ethanol phase splitting. With the knowledge of the phase behavior at these temperatures, the initial compositions of reagents could be selected to optimize the amount of solvent to be used and to guarantee the full miscibility of the mixture used in biodiesel production. Figure 4 shows the experimental points, tie lines, and binodal curve calculated using the NRTL model for the system containing refined canola oil (2) + anhydrous ethanol (4) + hexane (5) at (313.25 ± 0.1) K. As can be seen in Figure 4 and in Table 10, the NRTL model was also able to accurately describe the phase compositions for the studied systems with deviations of 0.47 % for the system at 313.25 K and 1.40 % for the system at 328.15 K. The evaluation of the global mass balance deviation indicated that the average errors were (0.08 and 0.09) % for the systems containing refined canola oil (2) + anhydrous ethanol (4) + hexane (5) at (313.25 ± 0.1) K and (328.15 ± 0.1) K, respectively, which confirms the good quality of the experimental data.

To compare results for the system containing refined canola oil + anhydrous ethanol + hexane at different temperatures, the experimental equilibrium data and binodal curves calculated by the NRTL model are shown in Figure 5. As occurred in the previous case the increase of temperature decreases the region of phase splitting.

Figures 6 and 7 show the equilibrium diagrams for the systems containing refined palm oil (3) + anhydrous ethanol (4) + hexane (5) at (318.15 ± 0.1) K and (328.25 ± 0.1) K, respectively. The NRTL model also describes correctly the experimental data for these systems, with an average deviation of (0.57 and 0.53) % (Table 10) for the systems at (318.15 ± 0.1) K and (328.25 ± 0.1) K, respectively. The deviation of the global mass balance was 0.16 % for the system at 318.15 K and 0.07 % for the system at 328.25 K confirming the good quality of the experimental data.

Conclusions

The results presented in this paper show that the NIR spectroscopy using multivariate calibration performed well in the determination of equilibrium data and can guarantee reliable results. The low uncertainties of the experimental data and the low deviation obtained in the global mass balance indicate the good quality of the equilibrium data for the systems of interest in biodiesel production at temperatures of (313.15, 318.15, and 328.15) K, containing different vegetable oils (soybean, canola, and palm oil) + anhydrous ethanol + hexane.

Acknowledgment

The authors wish to acknowledge Agropalma (Belém/PA, Brazil) for kindly supplying the refined palm oil.

Note Added after ASAP Publication: This paper was published ASAP on April 1, 2009. Changes were made to equation 8 and Table 9, and the revised paper was reposted on May 13, 2009. Additional changes were made to equation 8. The revised paper was reposted on June 11, 2009.

Literature Cited

(1) Pousa, G. P. A. G.; Santos, A. L. F.; Suarez, P. A. Z. History and Policy of Biodiesel in Brazil. *Energy Policy* **2007**, *35*, 5393–5398.

(2) Pinto, A. C.; Guarieiro, L. L. N.; Rezende, M. J. C.; Ribeiro, N. M.; Torres, E. A.; Lopes, W. A.; Pereira, P. A. P.; Andrade, J. B. Biodiesel: An Overview. *J. Braz. Chem. Soc.* **2005**, *16*, 1313–1330.

(3) Demirbas, A. Comparison of Transesterification Methods for Production of Biodiesel from Vegetable Oils and Fats. *Energy Conv. Manag.* **2008**, *49*, 125–130.

(4) Kucek, K. T.; César-Oliveira, M. A. F.; Wilhelm, H. M.; Ramos, L. P. Ethanolysis of Refined Soybean Oil Assisted by Sodium and Potassium Hydroxides. *J. Am. Oil Chem. Soc.* **2007**, *84*, 385–392.

(5) Meneghetti, S. M. P.; Meneghetti, M. R.; Wolf, C. R.; Silva, E. C.; Lima, G. E. S.; Silva, L. L.; Serra, T. M.; Cauduro, F.; Oliveira, L. G. Biodiesel from Castor Oil: A Comparison of Ethanolysis versus Methanolysis. *Energy Fuels* **2006**, *20*, 2262–2265.

(6) Lima, J. R. O.; Silva, R. B.; Moura, E. M.; Moura, C. V. R. Biodiesel of Tucum Oil, Synthesized by Methanolic and Ethanolic Routes. *Fuel* **2008**, *87*, 1718–1723.

(7) Hernández-Martín, E.; Otero, C. Different Enzyme Requirements for the Synthesis of Biodiesel: Novozym® 435 and Lipozyme® TL IM. *Bioresour. Technol.* **2008**, *99*, 277–286.

(8) Moreira, A. B. R.; Perez, V. H.; Zanin, G. M.; Castro, H. F. Biodiesel Synthesis by Enzymatic Transesterification of Palm Oil with Ethanol Using Lipases from Several Sources Immobilized on Silica-PVA Composite. *Energy Fuels* **2007**, *21*, 3689–3694.

(9) Oliveira, D.; Filho, I. N.; Di Luccio, M.; Faccio, C.; Dalla Rosa, C.; Bender, J. P.; Lipke, N.; Amroginski, C.; Dariva, C.; Oliveira, J. V. Kinetics of Enzyme-Catalyzed Alcoholysis of Soybean Oil in n-Hexane. *Appl. Biochem. Biotechnol.* **2005**, *121*, 231–242.

(10) Soumanou, M. M.; Bornscheuer, U. T. Improvement in Lipase-Catalyzed Synthesis of Fatty Acid Methyl Esters from Sunflower Oil. *Enzyme Microb. Technol.* **2003**, *33*, 97–103.

(11) Lanza, M.; Borges Neto, W.; Batista, E.; Poppi, R. J.; Meirelles, A. J. A. Liquid-Liquid Equilibrium Data for Reactional Systems of Ethanolysis at 298.3 K. *J. Chem. Eng. Data* **2008**, *53*, 5–15.

(12) Liu, X.; Piao, X.; Wang, Y.; Zhu, S. Liquid-Liquid Equilibrium for Systems of (Fatty Acid Ethyl Esters + Ethanol + Soybean Oil and Fatty Acid Ethyl Esters + Ethanol + Glycerol). *J. Chem. Eng. Data* **2008**, *53*, 359–362.

(13) Tizvar, R.; McLean, D. D.; Kates, M.; Dube, M. A. Liquid-Liquid Equilibria of the Methyl Oleate-Glycerol-Hexane-Methanol System. *Ind. Eng. Chem. Res.* **2008**, *47*, 443–450.

(14) Zhou, W.; Boocock, D. G. B. Phase Behavior of the Base-Catalyzed Transesterification of Soybean Oil. *J. Am. Oil Chem. Soc.* **2006**, *83*, 1041–1045.

(15) Zhou, W.; Boocock, D. G. B. Phase Distributions of Alcohol, Glycerol, and Catalyst in the Transesterification of Soybean Oil. *J. Am. Oil Chem. Soc.* **2006**, *83*, 1047–1052.

(16) Zhou, H.; Lu, H.; Liang, B. Solubility of Multicomponent Systems in the Biodiesel Production by Transesterification of *Jatropha curcas* L. Oil with Methanol. *J. Chem. Eng. Data* **2006**, *51*, 1130–1135.

(17) Barthus, R. C.; Poppi, R. J. Multivariate Quality Control Applied to Detect the Soybean Oil Oxidation Using Fourier Transform Infrared Spectroscopy. *Spectrosc. Lett.* **2002**, *35*, 729–739.

(18) Trevisan, M. G.; Garcia, C. M.; Schuchardt, U.; Poppi, R. J. Evolving Factor Analysis-Based Method for Correcting Monitoring Delay in Different Batch Runs for Use With PLS: On-Line Monitoring of a Transesterification Reaction by ATR-FTIR. *Talanta* **2008**, *74*, 971–976.

(19) Baptista, P.; Felizardo, P.; Menezes, J. C.; Correia, M. J. N. Multivariate Near Infrared Spectroscopy Models for Predicting the Methyl Esters Content in Biodiesel. *Anal. Chim. Acta* **2008**, *607*, 153–159.

(20) Felizardo, P.; Baptista, P.; Menezes, J. C.; Correia, M. J. N. Multivariate Near Infrared Spectroscopy Models for Predicting Methanol and Water Content in Biodiesel. *Anal. Chim. Acta* **2007**, *595*, 107–113.

(21) Pimentel, M. F.; Ribeiro, G. M. G. S.; Cruz, R. S.; Stragevitch, L.; Pacheco Filho, J. G. A.; Teixeira, L. S. G. Determination of Biodiesel Content When Blended With Mineral Diesel Fuel Using Infrared Spectroscopy and Multivariate Calibration. *Microchem J.* **2006**, *82*, 201–206.

(22) AOCS. *Official Methods and Recommended Practices of the American Oil Chemists' Society*, 3rd ed.; AOCS Press: Champaign, 1988; Vol. 1−2.

(23) Hartman, L.; Lago, R. C. A. Rapid Preparation of Fatty Acid Methyl Esters from Lipids. *Lab. Pract.* **1973**, *22*, 475–476.

(24) Antoniosi Filho, N. R.; Mendes, O. L.; Lanças, F. M. Computer Prediction of Triacylglycerol Composition of Vegetable Oils by HRGC. *Chromatographia* **1995**, *40*, 557–562.

(25) IUPAC. *Standard Methods for the Analysis of Oils, Fats and Derivatives, Part 1 (sections I and II)*, 6th ed.; Paquot, C., Ed.; Pergamon Press: New York, 1979.

(26) Silva, L. H. M.; Coimbra, J. S.; Meirelles, A. J. A. Equilibrium Phase Behavior of Poly(Ethylene Glycol) + Potassium Phosphate + Water Two Phase Systems at Various pH and Temperatures. *J. Chem. Eng. Data* **1997**, *42*, 398–401.

(27) Rodrigues, C. E. C.; Antoniassi, R.; Meirelles, A. J. A. Equilibrium Data for the System Rice Bran Oil + Fatty Acids + Ethanol + Water at 298.2 K. *J. Chem. Eng. Data* **2003**, *48*, 367–373.

(28) Geladi, P.; Kowalski, B. R. Partial Least Squares Regression: A Tutorial. *Anal. Chim. Acta* **1986**, *185*, 1–17.

(29) Brereton, R. G. Introduction to Multivariate Calibration in Analytical Chemistry. *Analyst* **2000**, *125*, 2125–2154.

(30) Otto, M. *Chemometrics: Statistics and Computer Application in Analytical Chemistry*; Wiley, 1999.

(31) Marcilla, A.; Ruiz, F.; García, A. N. Liquid-Liquid-Solid Equilibria of the Quaternary System Water-Ethanol-Acetone-Sodium Chloride at 25 °C. *Fluid Phase Equilib.* **1995**, *112*, 273–289.

(32) Rodrigues, C. E. C.; Silva, F. A.; Marsaioli, A., Jr.; Meirelles, A. J. A. Deacidification of Brazil Nut and Macadamia Nut Oils by Solvent Extraction: Liquid-Liquid Equilibrium Data at 298.2 K. *J. Chem. Eng. Data* **2005**, *50*, 517–523.

(33) Wilson, G. M. Vapor-Liquid Equilibrium XI: A New Expression for the Excess Gibbs Energy of Mixing. *J. Am. Chem. Soc.* **1964**, *86*, 127–130.

(34) Renon, H.; Prausnitz, J. M. Local Composition in Thermodynamic Excess Functions for Liquid Mixtures. *AIChE J.* **1968**, *14*, 135–144.

(35) Aznar, M. Correlation of (Liquid + Liquid) Equilibrium of Systems Including Ionic Liquids. *Braz. J. Chem. Eng.* **2007**, *24*, 143−149.

(36) Sé, R. A. G.; Aznar, M. Thermodynamic Modelling of Phase Equilibrium for Water + Poly(Ethylene Glycol) + Salt Aqueous Two-Phase Systems. *Braz. J. Chem. Eng.* **2002**, *19*, 255–266.

(37) Stragevitch, L. Liquid-Liquid Equilibrium in Non Electrolyte Mixtures, D.Sc. Thesis (in Portuguese), School of Chemical Engineering, State University of Campinas, Campinas, 1997.

(38) Zhao, J.; Jiang, X.-C.; Li, C.-X.; Wang, Z.-H. Vapor Pressure Measurement for Binary and Ternary Systems Containing a Phosphoric Ionic Liquid. *Fluid Phase Equilib.* **2006**, *247*, 190–198.

(39) Rodrigues, C. E. C.; Filipini, A.; Meirelles, A. J. A. Phase Equilibrium for Systems Composed by High Unsaturated Vegetable Oils + Linoleic Acid + Ethanol + Water at 298.2 K. *J. Chem. Eng. Data* **2006**, *51*, 15–21.

(40) Demirel, Y.; Paksoy, H. O. Calculations of Thermodynamic Derivative Properties from the NRTL and UNIQUAC Models. *Thermochim. Acta* **1997**, *303*, 129–136.

(41) Lee, M.-J.; Chang, Y.-K.; Lin, H.-m. Separation of 4-Morpholinepropanesulfonic Acid from Its Aqueous Solution. *Ind. Eng. Chem. Res.* **1997**, *36*, 5399–5402.

(42) Stragevitch, L.; d'Ávila, S. G. Application of a Generalized Maximum Likelihood Method in the Reduction of Multicomponent Liquid-Liquid Equilibrium Data. *Braz. J. Chem. Eng.* **1997**, *14*, 41–52.

(43) Null, H. R. *Phase Equilibrium in Process Design*; Wiley-Interscience: New York, 1970.

(44) Firestone, D. *Physical and Chemical Characteristics of Oils, Fats and Waxes*; AOCS Press, 1999.

Received for review December 12, 2008. Accepted February 21, 2009. The authors wish to acknowledge FAPESP (Fundação de Amparo à Pesquisa do Estado de São Paulo, 04/09591-2, and 05/53095-2), CNPq (Conselho Nacional de Desenvolvimento Científico e Tecnológico, 303649/2004-6), and CAPES (Coordenação de Aperfeiçoamento de Pessoal de Nível Superior) for their financial support.

JE800961A